Journal of Magnetic Resonance **140,** 32–40 (1999)
Article ID jmre.1999.1817, available online at http://www.idealibrary.com on IDEAL®

# Measurement of $^1J_{NC'}$ and $^2J_{HNC'}$ Couplings from Spin-State-Selective Two-Dimensional Correlation Spectrum

Perttu Permi,*[,1] Sami Heikkinen,* Ilkka Kilpeläinen,* and Arto Annila†

*Institute of Biotechnology, P.O. Box 56, University of Helsinki, FIN-00014, Helsinki, Finland; and
†VTT Chemical Technology, P.O. Box 1401, FIN-02044 VTT, Espoo, Finland

Received January 19, 1999; revised May 17, 1999

**A method for the measurement of $^1J_{NC'}$ and $^2J_{HNC'}$ coupling constants from a simplified two-dimensional [$^{15}$N, $^1$H] correlation spectrum is presented. The multiplet components of the $^1J_{NC'}$ doublet in the indirect dimension and $^2J_{HNC'}$ in the direct dimension are separated into two subspectra by spin-state-selective filters. Thus each subspectrum contains no more peaks than the conventional [$^{15}$N, $^1$H]-HSQC spectrum. Furthermore, the method for the measurement of $^1J_{NC'}$ and $^2J_{HNC'}$ is designed to exploit destructive relaxation interference (TROSY). The results are verified against the measurements of $^1J_{NC'}$ from spin-state-selective [$^{13}$C′, $^1$H] correlation spectra recorded with additional sequence described here.** 

*Key Words:* **coupling; spin-state-selective filters; TROSY; ubiquitin.**

## INTRODUCTION

Measurement of coupling constants for protein structure determination has remained of interest for several years. E.COSY (*1–5*), quantitative *J*-correlation (*6–10*), and traditional *J*-coupled (*11–13*) experiments have been employed to measure primarily $^3J$ scalar coupling constants related to dihedrals via Karplus relations. The traditional *J*-coupled methods provide an easy and accurate measurement of couplings but suffer from spectral crowding owing to the simultaneous presence of many multiplet components. To alleviate this overlap problem, editing with respect to a third dimension has been used (*4*). Also, recently spin-state-selective $\alpha/\beta$-filters have been devised to separate doublet components into two different subspectra (*14–24*). These methods have been implemented also in measurements of large heteronuclear one-bond couplings from proteins dissolved in weakly oriented liquid crystal phases to determine $^1J_{HN}$, $^1J_{NC'}$, and $^2J_{HNC'}$ with dipolar contributions using a $^{15}$N spin-state edited spectrum (*25*). The ease of extracting orientational information from one- and two-bond couplings, preferably from simplified two-dimensional spectra, is of an obvious importance.

In this paper, we show a straightforward but practical extension of the use of spin-state-selective filters to measure $^1J_{NC'}$ and $^2J_{HNC'}$ couplings from [$^{15}$N, $^1$H] correlation spectra in $^{15}$N/$^{13}$C-labeled proteins. We refer to this experiment as HN($\alpha/\beta$-NC′-*J*). In addition, we provide the selection for the [$^{15}$N, $^1$H] multiplet component with the most favorable relaxation properties (TROSY) (*18–22*). This method, referred as HN($\alpha/\beta$-NC′-*J*)-TROSY, is particularly amenable to perdeuterated proteins studied at high magnetic fields. We also introduce another method which allows the determination of $^1J_{NC'}$ from a two-dimensional spin-state-selective [$^{13}$C′, $^1$H] correlation spectrum as an attractive alternative for measurements at intermediate field strengths. We denote this experiment with the abbreviation H($\alpha/\beta$-NC′-*J*)CO. The original $\alpha/\beta$-filters (*14–24*) are modified for the present purpose to select carbonyl carbon or nitrogen spin-states. In the HN($\alpha/\beta$-NC′-*J*) correlation experiment in- and antiphase $^{15}$N–$^{13}$C′ magnetization are selected prior to the $t_1$ evolution period by the $\alpha/\beta$-filters with respect to $^1J_{NC'}$, whereas in the H($\alpha/\beta$-NC′-*J*)CO correlation experiment the in- and antiphase magnetization are edited with respect to $^1J_{HN}$. Similar to the S$^3$E -filter element, the undesired components of transverse magnetization are purged (*14, 15*). This allows the determination of two different couplings from a simplified spectrum with pure absorptive lineshapes.

## DESCRIPTION OF THE PULSE SEQUENCES

The HN($\alpha/\beta$-NC′-*J*) pulse sequence to measure $^1J_{NC'}$ and $^2J_{HNC'}$ (Fig. 1A) from a [$^{15}$N, $^1$H] correlation spectrum is based on the conventional [$^{15}$N, $^1$H]-HSQC experiment. Proton magnetization is first transferred into an antiphase heteronuclear single-quantum coherence between the amide proton and the nitrogen with the usual INEPT-step tuned to $1/(2J_{HN})$, followed by the $\alpha/\beta$-filter before the $t_1$ evolution period. In the first experiment, referred to as the antiphase experiment (filled 180° pulse on $^{13}$C′ and 90° pulse on $^{15}$N are applied), the heteronuclear coupling between the amide nitrogen and the adjacent carbonyl carbon evolves during the filter of length $1/(2J_{NC'})$ into an antiphase magnetization with respect to $^1J_{NC'}$. In the second experiment, referred to as the in-phase experiment (unfilled 180° pulses are applied on $^{13}$C′), $^{15}$N is effectively decoupled from $^{13}$C′. During the $t_1$ evolution period, the

[1] To whom correspondence should be addressed: Fax: +358-9-708 59541, E-mail: Perttu.Permi@helsinki.fi.



1090-7807/99 $30.00

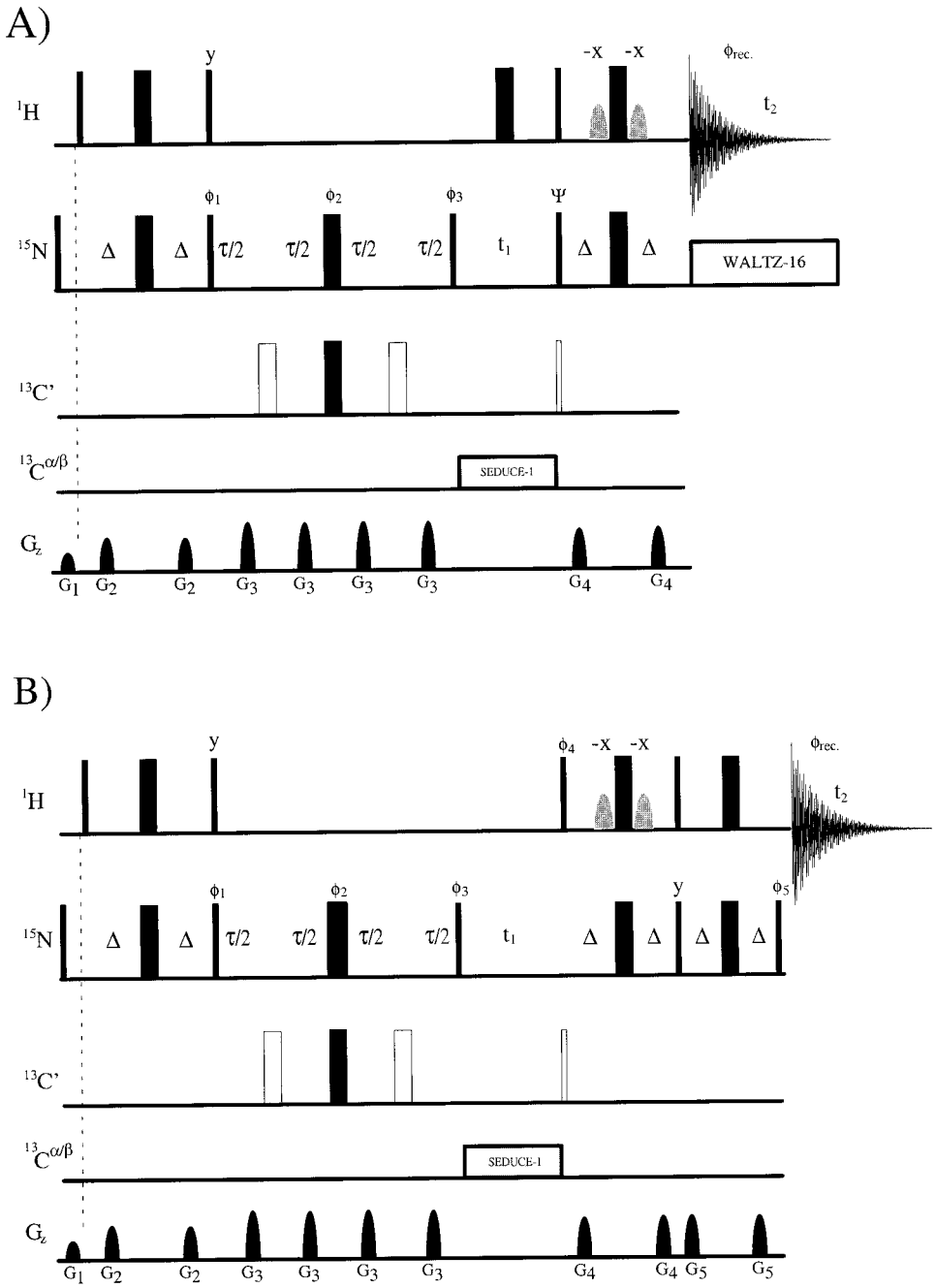


**FIG. 1.** Pulse sequences of the $\alpha/\beta$-filtered HN($\alpha/\beta$-NC′-*J*) experiment for the measurement of $^1J_{NC'}$ and $^2J_{HNC'}$ couplings from [$^{15}$N, $^1$H] correlation spectra. The sequences generate anti- and in-phase spectra. Hard 90° and 180° pulses are marked by (un)filled narrow and wide bars, respectively, with the phase *x*, unless indicated otherwise. Selective 90° pulses of the WATERGATE solvent suppression scheme (*31*) are shown as gray half ellipses. If only $^1J_{NC'}$ is desired, an optional 90° purge pulse (indicated with an unfilled narrow bar) on the carbonyl carbon after the $t_1$ evolution period can be applied. Aliphatic carbons are selectively decoupled during $t_1$ with SEDUCE-1 (*32*) and nitrogens during acquisition with WALTZ-16 (*33*). Delay durations: $\Delta = 1/(4J_{HN})$, $\tau = 1/(4J_{NC'})$. (A) phase cycling for the antiphase spectrum: $\phi_1 = 2(x, -x)$; $\phi_2 = 4(x)$; $\phi_3 = 2(x)$, $2(-x)$; $\phi_{rec} = 2(x, -x)$, and $\psi = 4(y)$. The phases $\phi_1$, $\phi_2$, and $\phi f_3$ are incremented in States–TPPI manner (*34*). Phase cycling for the in-phase spectrum: $\phi_1 = 2(x, -x)$; $\phi_2 = 4(x)$; $\phi_{rec} = 2(x, -x)$ and $\psi = 4(x)$. The phases $\phi_1$ and $\phi_2$ are incremented in States–TPPI manner. (B) Pulse sequence of the $\alpha/\beta$-filtered HN($\alpha/\beta$-NC′-*J*) experiment for the measurement of $^1J_{NC'}$ and $^2J_{HNC'}$ couplings from [$^{15}$N, $^1$H] correlation spectra with the generalized TROSY. Phase cycling for the antiphase spectrum: $\phi_1 = 2(, -x)$; $\phi_2 = x$; $\phi_3 = 2(x)$, $2(-x)$ and $\phi_{rec} = 2(x, -x)$. Phase cycling for the in-phase spectrum: $\phi_1 = 2(y, -y)$; $\phi_2 = y$; $\phi_{rec} = 2(x, -x)$. The phases $\phi_1$, $\phi_2$, and $\phi_3$ are incremented in States–TPPI manner (*34*). The addition and subtraction of these two spectra result in up- and downfield $^{15}$N–$^{13}$C′ multiplet components. For $^{15}$N–$^1$H multiplet selection, four different data sets are recorded (I): $\phi_4 = y$; $\phi_5 = x$, (II): $\phi_4 = -y$; $\phi_5 = -x$, (III): $\phi_4 = -y$; $\phi_5 = x$, and (IV): $\phi_4 = y$; $\phi_5 = -x$. The addition and subtraction of data sets (I) and (II) result in two intermediate data sets (I + II) and (I − II). Finally, a single multiplet component is selected by addition or subtraction of the intermediate data set (I + II) with the data set (I − II) shifted by 90° in both dimensions. The data sets (III) and (IV) are handled in a completely analogous way. For detailed instructions see Ref. (*20*).

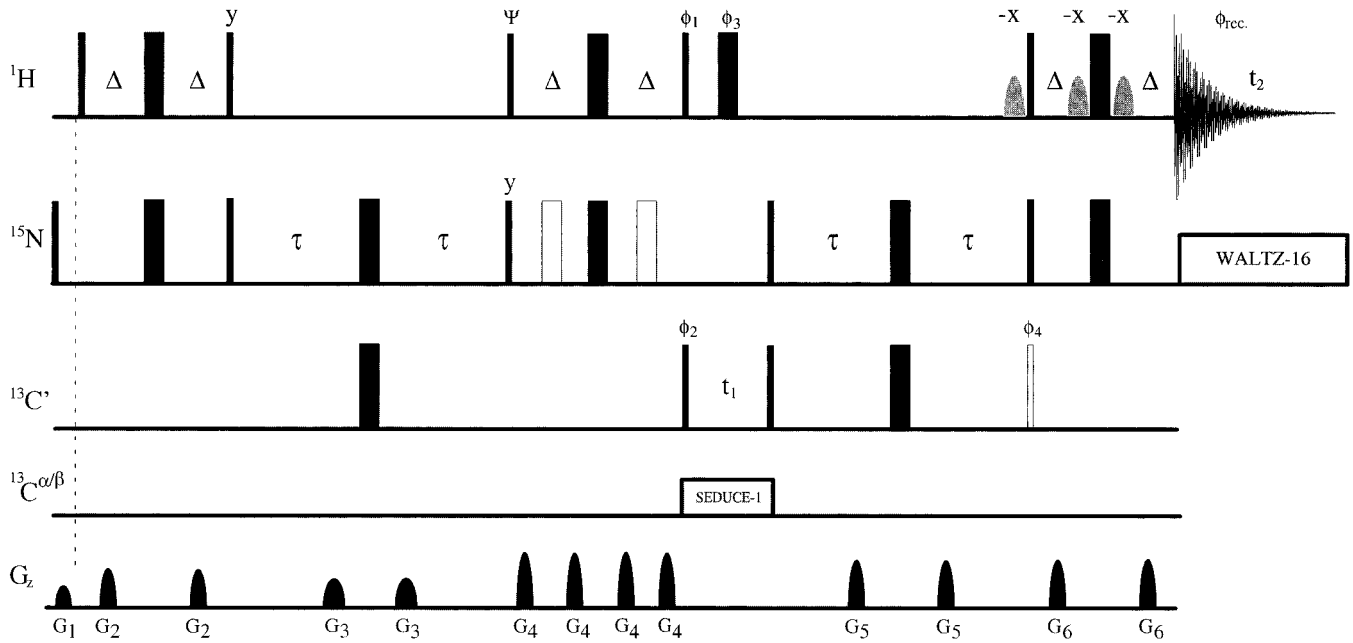


**FIG. 2.** Pulse scheme of the spin-state-selective H($\alpha/\beta$-NC′-*J*)CO experiment for the measurement of $^1J_{NC'}$ couplings from [$^{13}$C′, $^1$H] correlation spectra. An optional 90° pulse (indicated with an unfilled narrow bar) on the carbonyl carbon after the second $2\tau$ period can be used to purge undesired components. Aliphatic carbons are selectively decoupled during $t_1$ with SEDUCE-1 (*32*) and nitrogens during acquisition with WALTZ-16 (*33*). Pulses (180°) on $^{13}$C′ are applied selectively with strength of $\delta/\sqrt{3}$, where $\delta$ is the frequency between the center of the $^{13}$C′ and $^{13}C^{\alpha}$ spectral region. Delay durations: $\Delta = 1/(4J_{HNN})$, $\tau = 1/(4J_{NC'})$. The phase $\phi_2$ is incremented in States–TPPI manner to give frequency discrimination in $F_1$-dimension (*34*). Phase cycling for $\sin(\omega_{C'}t_1)\sin(\pi J_{NC'}t_1)$ modulated data: $\phi_1 = 2(y, y, -y, -y)$; $\phi_2 = 4(x, -x)$; $\phi_3 = 4(x), 4(-x)$; ($\phi_4 = 8(x), 8(-x)$); $\psi = 8(x)$ and $\phi_{rec} = 2(x, -x, -x, x)$. For $\cos(\omega_{C'}t_1)\cos(\pi J_{NC'}t_1)$ modulated data $\psi = 8(y)$. The addition and subtraction of the in- and antiphase spectra result in up- and downfield multiplet components.

$^{15}$N chemical shift and $^1J_{NC'}$ are active. Aliphatic carbons are decoupled in the course of $t_1$ incrementation. During the acquisition amide nitrogens are decoupled but the $^2J_{HNC'}$ couplings remain active. The signal of interest described by the product operator formalism (*26*) neglecting relaxation is, prior to acquisition, proportional to

$$H_x\sin(2\pi J_{NC'}\tau)\sin(\omega_N t_1)\sin(\pi J_{NC'}t_1) + 2H_xC_z'\sin(2\pi J_{NC'}\tau)\cos(\omega_N t_1)\cos(\pi J_{NC'}t_1)$$

for the antiphase experiment, and to

$$H_x\cos(\omega_N t_1)\cos(\pi J_{NC'}t_1) + 2H_xC_z'\sin(\omega_N t_1)\sin(\pi J_{NC'}t_1)$$

for the in-phase experiment. Thus, the antiphase experiment results in antiphase and the in-phase experiment yields in-phase cross peaks with respect to $^1J_{NC'}$ in the $F_1$ domain and $^2J_{HNC'}$ in the $F_2$ domain. The cross peaks for the $\alpha$- and $\beta$-states of $^{13}$C′ are readily processed to two subspectra by the addition and subtraction of the antiphase and in-phase spectra either in the time or the frequency domain.

The 90° pulse on nitrogen before the $t_1$ evolution in the antiphase experiment serves to purge the component of magnetization which originates from the *J*-mismatch of the filter. The preferred sine-modulated magnetization is not affected by the aforementioned pulse whereas the undesirable cosine-modulated term is converted into a longitudinal two-spin order which is not transformed into an observable proton magnetization by the subsequent events. In the in-phase experiment, the heteronuclear coupling is not active during the $\alpha/\beta$-filter element and purging is not essential. Thus, the antiphase and in-phase experiments will yield antiphase and in-phase E.COSY-like tilted cross peak patterns, respectively, from which $^1J_{NC'}$ and $^2J_{HNC'}$ can be measured in the $F_1$ and $F_2$ dimensions, respectively. Obviously, either one of the experiments would provide the two heteronuclear coupling constants in much the same way as a $^{13}$C′-coupled [$^{15}$N, $^1$H]-HSQC spectrum (*13*) but the addition and the subtraction of the antiphase and in-phase spectra will result in two simplified subspectra edited with respect to the $^{13}$C′ spin-state. Each subspectrum has no more cross peaks than a conventional [$^{15}$N, $^1$H]-HSQC spectrum. Optionally, only the $^1J_{NC'}$ coupling could be recorded by applying a 90° pulse on the $^{13}$C′ spins after the $t_1$ evolution to remove any $^{13}$C′ *z*-magnetization. Alternatively, the carbonyl carbons could be decoupled during the acquisition to remove the $^2J_{HNC'}$ couplings. Furthermore, the spin-state selection could be applied with respect to $^1J_{HNN}$ along $F_2$ as described by Andersson *et al.* (*16, 17*). Thus, three couplings $^1J_{NC'}$, $^2J_{HNC'}$, and $^1J_{HNN}$ could be measured from the spectra

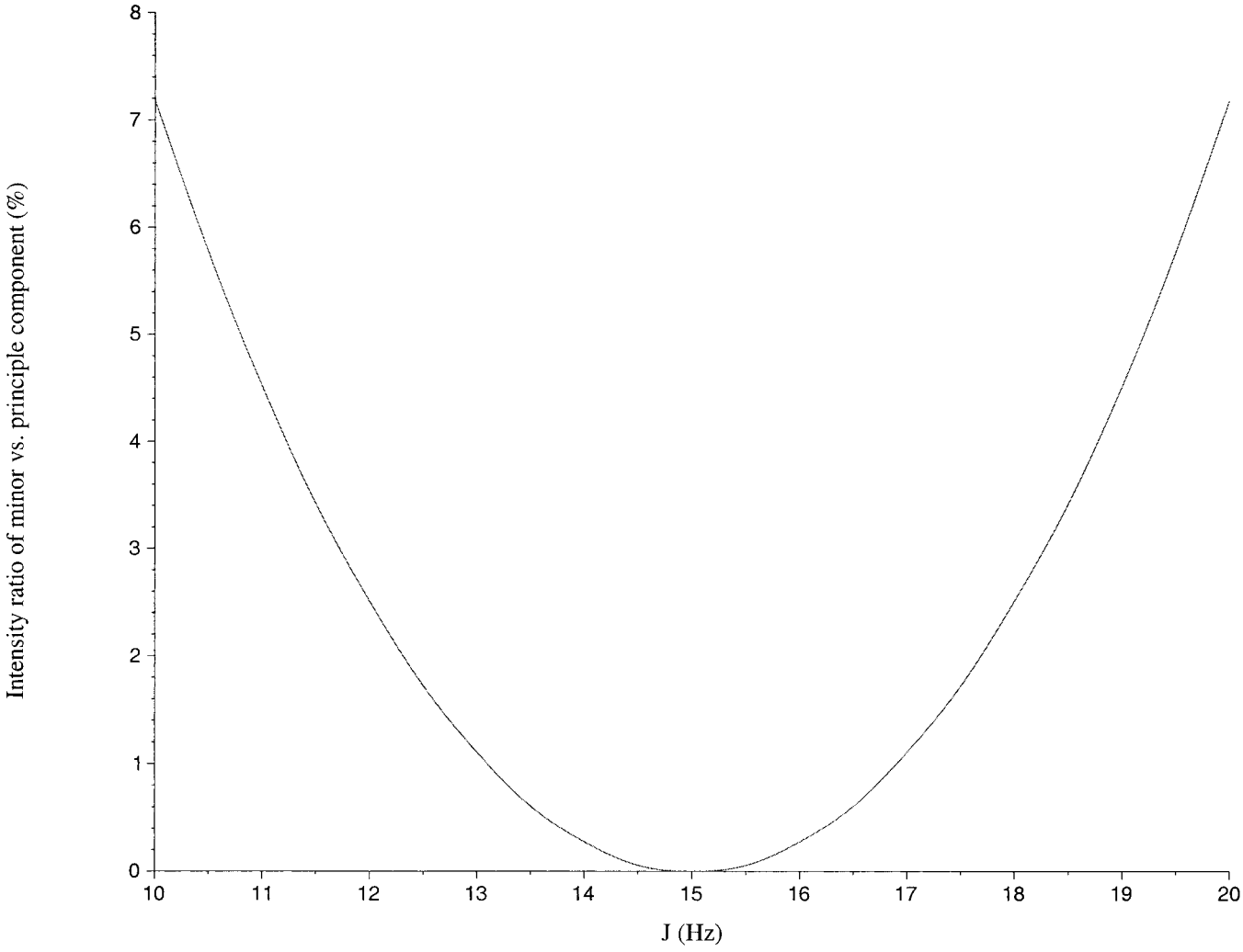


**FIG. 3.** Intensity (%) of the minor component relative to the principle component as a function of $J$. The plot was calculated using 15 Hz as a nominal value for $^1J_{NC'}$. In the interval from 11.6 to 18.4 Hz the ratio of the principle to the minor component is at least 30 which guarantees good filtering.

without introducing additional crowding compared with an HSQC spectrum.

For large proteins at high magnetic fields transverse relaxation optimized spectroscopy (TROSY) improves sensitivity and resolution (*18–22*). Implementation of the generalized TROSY scheme (*20–22*) into the HN($\alpha/\beta$-NC′-$J$) sequence is shown in Fig. 1B. The generalized HN($\alpha/\beta$-NC′-$J$)-TROSY, if desired, provides, in addition to improved sensitivity and resolution, an option to measure $^1J_{HNN}$ couplings from the same data set.

At intermediate field strengths an alternative to the HN($\alpha/\beta$-NC′-$J$) is the H($\alpha/\beta$-NC′-$J$)CO experiment (Fig. 2), which is a modification of the HNCO pulse scheme (*26*). In this case, the $^1J_{NC'}$ values are measured from the $^{13}$C′-dimension in the [$^{13}$C′, $^1$H] correlation spectrum. The H($\alpha/\beta$-NC′-$J$)CO experiment begins with the usual $^1$H, $^{15}$N INEPT transfer step, which is followed by a heteronuclear spin-echo period during which the $^{15}$N coherence dephases with respect to the preceding $^{13}$C′ spin. In the course of the subsequent filter period, the coupling between $^1H^N$ and $^{15}$N is active in the antiphase experiment (filled 180° pulse on $^{15}$N is applied), while it is effectively decoupled in the in-phase experiment (unfilled 180° pulses on $^{15}$N are applied). Thus, a $^{13}$C′ coherence described by an operator $2H_z^NC'_y$ is created before the $t_1$ evolution period in the antiphase filter while the coherence proportional to a term $4H_z^NN_zC'_y$ is created in the in-phase filter. Chemical shift of $^{13}$C′ evolves simultaneously with $^1J_{NC'}$ during $t_1$ and the signal of interest at the end of the $t_1$ period is proportional to $4H_z^NN_zC'_y\sin(2\pi J_{HNN}\Delta)\sin(\omega_{C'}t_1)\sin(\pi J_{NC'}t_1)$ and $4H_z^NN_zC'_y\cos(\omega_{C'}t_1)\cos(\pi J_{NC'}t_1)$ for the antiphase and the in-phase spectrum, respectively. Postacquisitional addition and subtraction of these two experiments and their corresponding quadrature counterparts result in upfield and downfield doublet components. Obviously, $^1J_{NC'}$ can be extracted directly from the difference of the $^{13}$C′ chemical shifts of corresponding resonances in the two subspectra. After labeling of the $^{13}$C′ frequencies, magnetization is transferred back to nitrogen and finally to amide proton by a reverse INEPT step. For the

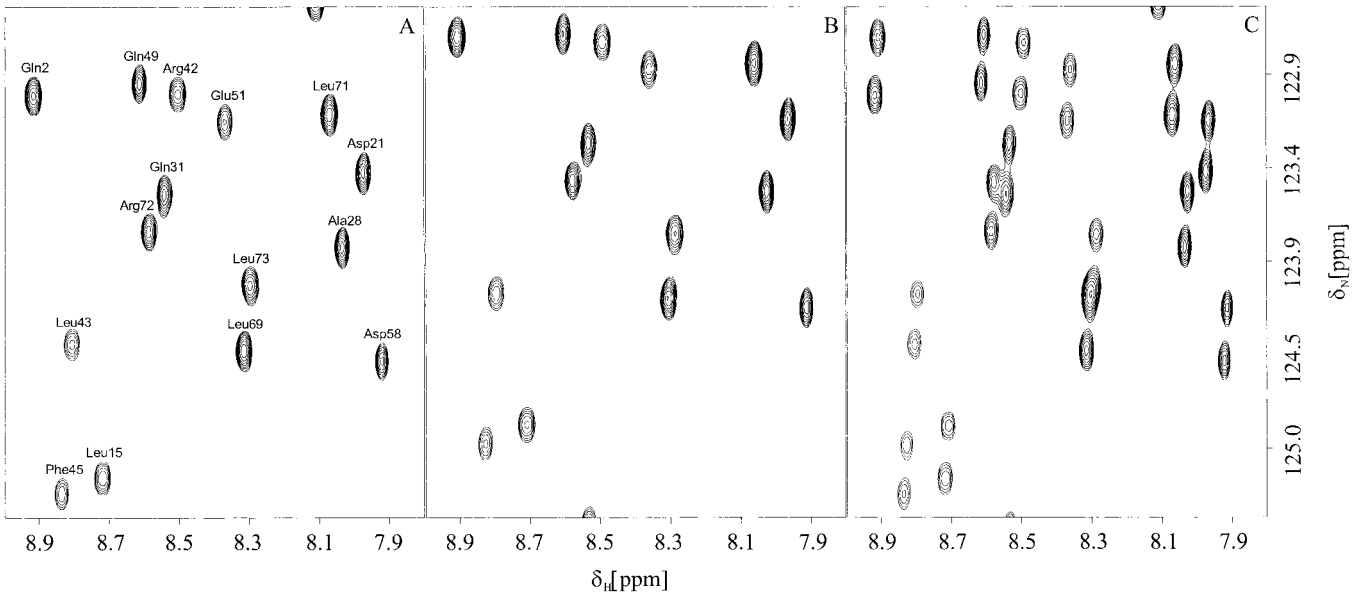


**FIG. 4.** Expansions of the $\alpha/\beta$-filtered spectra of ubiquitin recorded with pulse sequences in Fig. 1. Addition and subtraction of the anti- and in-phase components result in downfield (A) and upfield (B) components. As a reference, $^{13}C'$-coupled [$^{15}N$, $^{1}H$]-HSQC spectrum (C) was recorded. Sample conditions: 1.0 mM uniformly $^{15}N/^{13}C$-labeled human ubiquitin from VLI Research (76 residues, 8.6 kDa), dissolved in 90/10% $H_2O/D_2O$ in Wilmad 535PP NMR tube, pH 5.8, 50 mM phosphate buffer. Spectra were acquired at 30°°C with a Varian Unity 500 spectrometer equipped with a pulsed field gradient unit and a triple resonance probe head with an actively shielded $z$-axis gradient. Experimental parameters for the $\alpha/\beta$-filtered experiments: gradient strengths (durations): $G_1$ = 4.0 (0.7); $G_2$ = 10.0 (0.7); $G_3$ = 8.0 (0.7); $G_4$ = 15.6 G/cm (0.7 ms). Gradient recovery time = 200 $\mu$s. Delay durations: $\Delta$ = 2.7 ms, $\tau$ = 16.6 ms. The selective 90° proton pulse was a 1.18-ms rectangular pulse applied to the water resonance. Selective decoupling of aliphatic carbons with SEDUCE-1 was generated with the Pandora's Box software package (*35*). Spectral widths in $F_1$ ($F_2$) dimension = 1700 (8000) Hz, number of $t_1$ increments = 256, acquisition time ($t_2$) = 128 ms, number of scans = 64. Data were zero-filled to 2 K (8 K) in $F_1(F_2)$ dimension; squared cosine window functions were applied in the $F_1$ and $F_2$ dimensions. Data were processed with the Felix97.0 software package (*36*).

antiphase spectrum, the phase of the $\psi$ pulse is shifted by 90° with respect to the in-phase experiment. The $\phi_4$-pulse on carbonyl carbon serves to purge undesired magnetization components.

## RESULTS AND DISCUSSION

Cross-correlation between dipole–dipole (DD) and chemical shift anisotropy (CSA) relaxation mechanisms usually causes different relaxation rates for the two $^{15}N$ doublet components (*28*). The $\alpha/\beta$-filters used in the presented experiments are insensitive to this as the carbonyl carbon spin-state is inverted during the filter element. Therefore, the $\alpha$- and $\beta$-components of the $^{15}N$–$^{13}C'$ doublet relax at the same rate with respect to CSA and dipolar contributions. Nevertheless, due to the different relaxation properties of the antiphase ($4H_zN_xC_z'$) and in-phase ($2H_zN_y$) magnetizations in the HN($\alpha/\beta$-NC′-$J$) experiments, the amplitude of the sine-modulated antiphase magnetization is slightly smaller than the cosine-modulated in-phase magnetization. Ignoring other relaxation mechanisms during the $\alpha/\beta$-filter, the antiphase and in-phase operators relax at rates given by Eq. [1].

$$R_2(H_z^N N_x C_z') = R_2(^{15}N) + R_1(^{1}H^N) + R_1(^{13}C');$$
$$R_2(H_z^N N_y) = R_2(^{15}N) + R_1(^{1}H^N). \quad [1]$$

Analogously, corresponding relaxation rates for the H($\alpha/\beta$-NC′-$J$)CO experiment are

$$R_2(H_z^N N_z C_y') = R_2(^{13}C') + R_1(^{1}H^N) + R_1(^{15}N);$$
$$R_2(H_z^N C_y') = R_2(^{13}C') + R_1(^{1}H^N). \quad [2]$$

In principle, these differences in the relaxation rates could lead to an imperfect $\alpha/\beta$-filtering as a fraction of the doublet component in the $\alpha$-state would be present in the $\beta$-state selective subspectrum and vice versa. In the case of large proteins, the mismatch in the relaxation rates at high magnetic fields could be corrected for by scaling the antiphase and in-phase spectra before the construction of the subspectra as suggested by Ottiger *et al.* and Sørensen *et al.* (*23*, *29*).

In addition, HN($\alpha/\beta$-NC′-$J$) experiments, as all E.COSY -type experiments, are prone to $J$ crosstalk due to passive spin flips. If the passive spin, $^{13}C'$ in this case, changes its spin-state between the evolution and acquisition periods, the values measured from the $^{2}J_{HNC'}$ splitting will be slightly inaccurate. This phenomenon and methods for its compensation have been recently discussed by Sørensen *et al.* and Meissner *et al.* (*29*, *30*). In this particular case, the spin flip rate of $^{13}C'$ is relatively slow and subspectral editing is only slightly affected

**TABLE 1**

| | HN($\alpha/\beta$-NC′-$J$) | | $^{13}$C′-coupled HSQC | |
|---|---|---|---|---|
| Residue | $^1J_{NC'}$ [Hz] | $^2J_{HNC'}$ [Hz] | $^1J_{NC'}$ [Hz] | $^2J_{HNC'}$ [Hz] |
| Gln2 | 16.5 | 4.5 | 16.4 | 4.4 |
| Leu15 | 15.0 | 4.8 | 14.9 | 4.8 |
| Asp21 | 14.6 | 4.2 | 14.4 | 4.2 |
| Ala28 | 15.8 | 4.0 | 15.7 | 4.1 |
| Gln31 | 14.3 | 4.4 | 14.2 | 4.5 |
| Arg42 | 14.7 | 5.0 | 14.5 | 4.9 |
| Leu43 | 14.4 | 4.9 | 14.3 | 4.9 |
| Phe45 | 14.0 | 4.2 | 13.8 | 4.2 |
| Gln49 | 13.7 | 4.2 | 13.6 | 4.1 |
| Glu51 | 14.7 | 4.3 | 14.5 | 4.3 |
| Asp58 | 15.0 | 4.1 | 14.9 | 4.0 |
| Leu69 | 14.7 | 4.4 | — | — |
| Leu71 | 14.7 | 4.4 | 14.6 | 4.3 |
| Arg72 | 14.3 | 3.9 | 14.2 | 4.0 |
| Leu73 | 14.8 | 5.2 | — | — |

*Note.* Measured $^1J_{NC'}$ and $^2J_{HNC'}$ coupling constants for the residues shown in Fig. 4, recorded with the HN($\alpha/\beta$-NC′-$J$) pulse sequence and with the $^{13}$C′-coupled [$^{15}$N, $^1$H]-HSQC as the reference. Due to resonance overlap, coupling constants could not be measured for Leu[69] and Leu[73] from the $^{13}$C′-coupled [$^{15}$N, $^1$H]-HSQC spectrum of ubiquitin.

by $^{13}$C′ spin flips between the $t_1$ and $t_2$ periods, and errors in the measured $^2J_{HNC'}$ coupling constants will remain small.

The sensitivity of the employed $\alpha/\beta$-filters to the $J$-mismatch in the HN($\alpha/\beta$-NC′-$J$) experiment is the same as in the original version (*17*), except for the minute signal loss due to the chemical shift evolution during the 90° purge pulse in the antiphase filter element. Figure 3 shows the intensity of the minor component relative to the principle component as a function of $J$ when the filter delay is tuned to a nominal value of $^1J_{NC'}$, i.e., 15 Hz. A clean separation of multiplet components into subspectra can be obtained when $J$ values fall between 11.6 and 18.4 Hz. Within this interval the intensity of the minor component, arising from the $J$ mismatch, is at least 30 times smaller than the intensity of the principle component. This is superfluous for scalar $^1J_{NC'}$ couplings which usually deviate no more than $\pm$1.5 Hz from 15 Hz. Larger deviations from the tuned coupling are expected in anisotropic phase due to residual dipolar contributions. However, owing to the low gyromagnetic ratios of nitrogen and carbon, these contributions remain quite small, e.g., $\leq$2 Hz, when the maximal dipolar contribution to $^1J_{HNN}$ coupling is approximately 15 Hz. Larger values of residual dipolar couplings will limit the polarization transfers as well. Considering an extreme case, where scalar coupling is 13 Hz and dipolar contribution to the splitting is $-2$ Hz resulting in $^1J + D = 11$ Hz, the crosstalk is likely to be substantial. The artifact can be corrected by the appropriate scaling of the in- and antiphase data in the construction of subspectra (*23, 29, 30*). Especially with larger proteins, the degree of $J$ crosstalk may not be easily estimated due to overlapping doublet components. Therefore, besides the sensitivity reasons, the HN($\alpha/\beta$-NC′-$J$)-TROSY spectra allow a more accurate estimation of the appropriate scaling factors for the antiphase and in-phase spectra. Thus, in practice when $J$ mismatch is considered, the presented filter scheme is sufficient for subspectral editing in both isotropic and anisotropic media.

As is commonly known, a measurement of coupling from a partially resolved in-phase doublet will give an underestimate of the coupling constant. In the case of $\alpha/\beta$-filtered experiments, the estimation of $^1J_{NC'}$ coupling constants will also be inaccurate if the subspectral editing is incomplete. This raises from the fact that the undesired minor component will shift the apparent position of the desired principle component leading to incorrect separation of peaks in different subspectra. In any case, the apparent peak placements deviate less from their true positions due to the residual crosstalk artifact possibly remaining after the scaling operation than the overlapping in-phase multiplet components in the conventional $^{13}$C′-coupled HSQC experiment.

The variation of the $^1J_{NC'}$ couplings is percentually larger than that of the $^1J_{HNN}$ couplings. Consequently the $J$ crosstalk may arise from a $J$ mismatch in the presence of residual dipolar couplings (*vide supra*). In this respect the main advantage of the H($\alpha/\beta$-NC′-$J$)CO experiment over HN($\alpha/\beta$-NC′-$J$) is the very robust filter element. The editing is based on a large $^1J_{HNN}$ coupling, which is quite uniform through all residues in the protein backbone. Consequently, the editing in the H($\alpha/\beta$-NC′-$J$)CO experiment is insensitive to the $J$ mismatch even in the presence of large residual dipolar contributions and excellent filtering can be expected also for those residues where $^1J_{NC'}$ coupling deviates excessively ($>\pm$1.5 Hz) from the nominal 15 Hz, which might compromise the subspectral editing in the HN($\alpha/\beta$-NC′-$J$) experiment.

The method for the determination of $^1J_{NC'}$ and $^2J_{HNC'}$ from the spin-state-selective subspectra was demonstrated for 8.6-kDa (76 residues) uniformly $^{15}$N/$^{13}$C-labeled human ubiquitin (VLI Research, Southeastern, PA). Representative expansions of the $\alpha/\beta$-filtered $^1J_{NC'}$ and $^2J_{HNC'}$ subspectra of ubiquitin are shown in Figs. 4A and 4B, recorded with the pulse sequences in Fig. 1A together with the $^{13}$C′-coupled [$^{15}$N, $^1$H]-HSQC (*13*) spectrum (C) as reference.

The spectrum in Fig. 4A presents downfield components of the $^{15}$N–$^{13}$C′ doublet, whereas upfield components are in the spectrum in Fig. 4B. There are no signs of significant artifacts resulting from the addition and subtraction in these subspectra. The good quality of the aforementioned suppression arises from the insensitivity of the filter to the $J$-mismatch and from the similar relaxation rates of the anti- and in-phase components, implying that $R_1(^{13}C')$ is small, as expected. For reference, both $^{15}$N–$^{13}$C′ doublet components are in-phase in the spectrum in Fig. 4C, split by the $^1J_{NC'}$ coupling in the $F_1$ dimension and by $^2J_{HNC'}$ in the $F_2$ dimension. Measured $^1J_{NC'}$ and $^2J_{HNC'}$ values for residues shown in Fig. 4 are listed in Table 1.

Measured coupling constants agree well (deviation $\leq$0.2 Hz) with those obtained using the $^{13}$C′-coupled [$^{15}$N, $^1$H]-

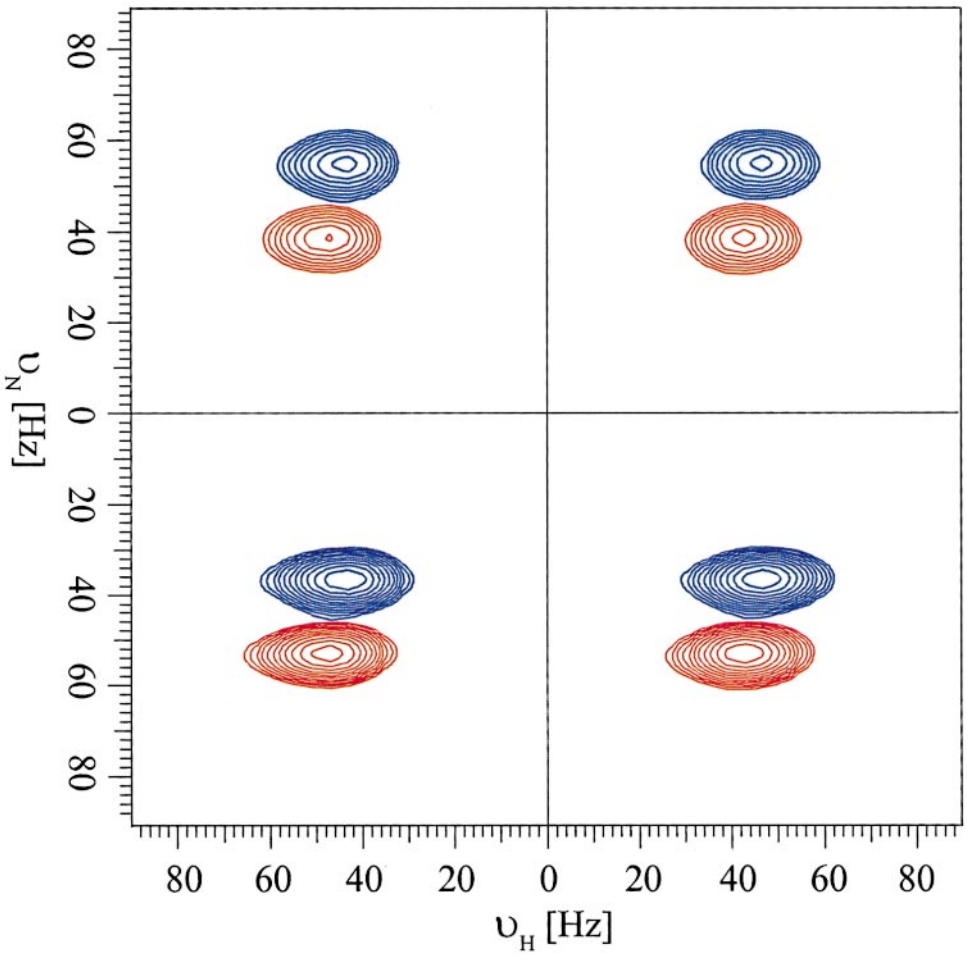


**FIG. 5.** Expansions of four $^{1}H^{N}$–$^{15}N$ multiplets of Ile36 $^{15}N$–$^{13}C'$ doublet recorded with the generalized HN($\alpha/\beta$-NC′-*J*)-TROSY pulse sequence. The $^{1}H^{N}$–$^{15}N$ cross peak at the bottom right corner represents the most slowly relaxing component. For each $^{1}H^{N}$–$^{15}N$ cross peak downfield (red contours) and upfield (blue contours) $^{15}N$–$^{13}C'$ doublet components of the subspectra are overlaid. Sample conditions are as in Fig. 4. The spectrum was acquired at 25°C with a Varian Unity 600 spectrometer equipped with a pulsed field gradient unit and a triple resonance probe head with an actively shielded *z*-axis gradient. Experimental parameters are as in Fig. 4 except for gradient strengths (durations): $G_5$ = 17.7 G/cm (0.7 ms), spectral widths in $F_1$ ($F_2$) dimension = 1800 (8000) Hz, acquisition time ($t_2$) = 256 ms, and number of scans = 8. Data were zero-filled to 4 K (4 K) in $F_1$ ($F_2$) dimension, squared cosine window functions were applied in the $F_1$ and $F_2$ dimensions.

HSQC. Nevertheless, there seems to be a tendency for slightly larger coupling constants measured from the $\alpha/\beta$-filtered subspectra than from the $^{13}C'$-coupled [$^{15}N$, $^{1}H$]-HSQC spectrum. This can be understood by the principles discussed earlier, i.e., the two doublet components overlap in the $^{13}C'$-coupled [$^{15}N$, $^{1}H$]-HSQC spectrum and measured coupling constants are underestimations of the true coupling constants. In the case of the HN($\alpha/\beta$-NC′-*J*) experiment, each subspectrum contains only one of the doublet components and cross peak placements are not shifted toward each other as in the $^{13}C'$-coupled [$^{15}N$, $^{1}H$]-HSQC, resulting in larger coupling constants.

Figure 5 shows four expansions of the downfield (red) and upfield (blue) components of the $^{15}N$–$^{13}C'$ doublet of Ile36 in the generalized HN($\alpha/\beta$-NC′-*J*)-TROSY spectrum. The component in the lower right corner represents the slowest relaxing $^{1}H^{N}$–$^{15}N$ multiplet component. At the field of 600 MHz line narrowing due to destructive relaxation interference of DD and CSA interactions in the $^{15}N$ dimension is quite small.

A representative expansion of the downfield (A) and upfield (B) components of the $^{15}N$–$^{13}C'$ doublet, obtained using the H($\alpha/\beta$-NC′-*J*)CO experiment, shown in Fig. 6, exemplifies the excellent separation of the $\alpha$- and $\beta$-states into different subspectra. There is no sign of *J* crosstalk in either subspectrum.

Coupling constants determined from the H($\alpha/\beta$-NC′-*J*)CO spectrum were compared with those obtained from the HN($\alpha/\beta$-NC′-*J*)-TROSY experiment at 600 MHz. A good correlation between $^{1}J_{NC'}$ coupling constants measured from these two experiments was found (Fig. 7). The pairwise root-mean-squared deviation is 0.13 Hz for the 69 residues considered.

Favorable relaxation properties of carbonyl carbon spin at low magnetic fields (<600 MHz) make the H($\alpha/\beta$-NC′-*J*)CO scheme a convenient alternative to the HN($\alpha/\beta$-NC′-*J*) exper-

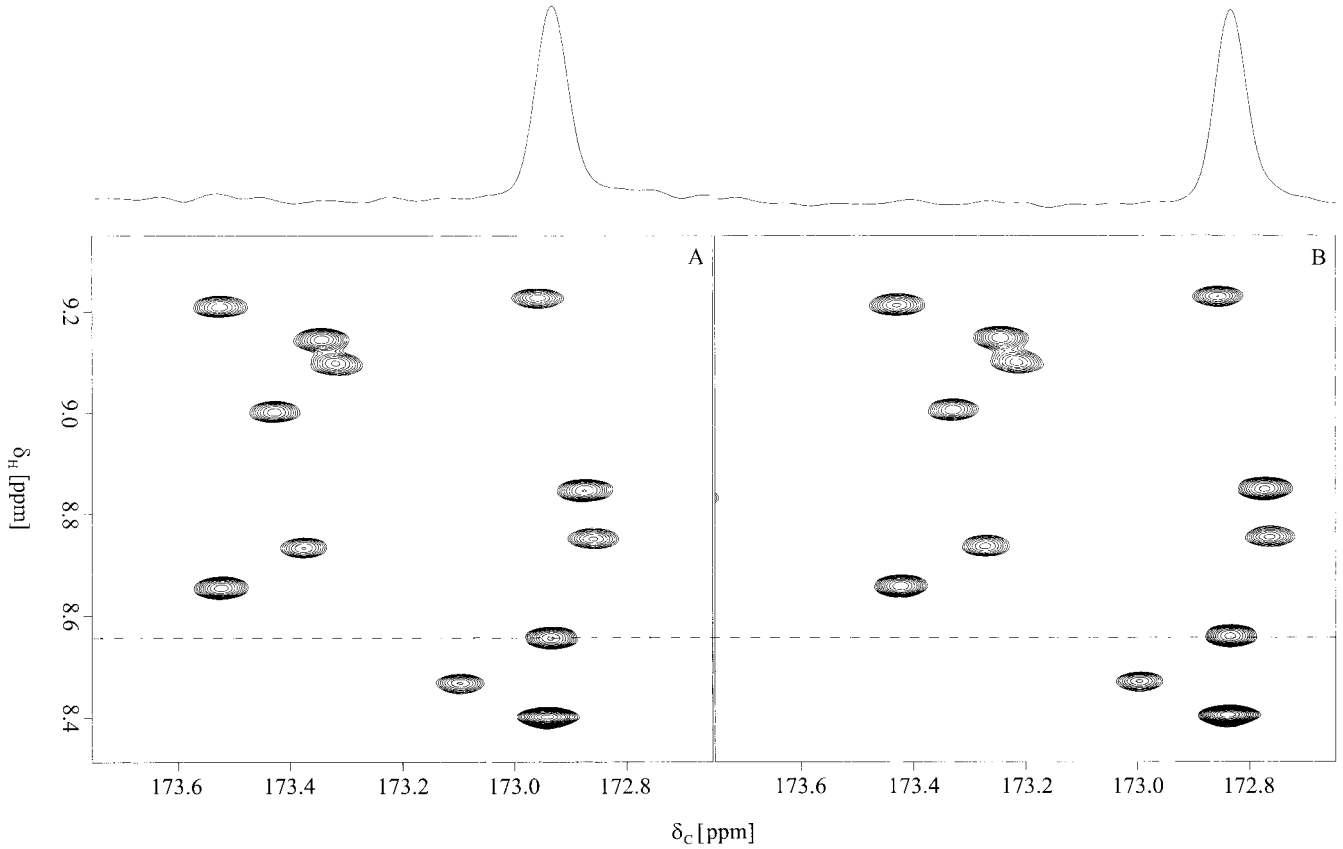


**FIG. 6.** Expansion of the [$^{13}$C′–{$^{15}$N},$^{1}$H] correlation spectrum obtained with H($\alpha/\beta$-NC′-*J*)CO pulse sequence (Fig. 2). The downfield (A) and upfield (B) components of the $^{15}$N–$^{13}$C′ doublet were obtained by postacquisitional addition and subtraction of antiphase and in-phase data sets in the frequency domain. The dashed line indicates the corresponding cross-section shown above. Spectra were acquired with a Varian Unity 600 spectrometer at 25°C. Gradient strengths (durations): $G_1$ = 4.0 (0.7); $G_2$ = 10.0 (0.7); $G_3$ = 7.0 (0.7); $G_4$ = 12.5 $\mu$s (0.7 $\mu$s), $G_5$ = 9.0 $\mu$s (0.7 $\mu$s); $G_6$ = 16 G/cm (0.7 ms). Gradient recovery time = 200 $\mu$s. Delay durations: $\Delta$ = 2.75 ms, $\tau$ = 16.6 ms. Selective decoupling of aliphatic carbons with SEDUCE-1 was generated with the Pandora's Box software package (*35*). Spectral widths in $F_1$ ($F_2$) dimension = 1800 (8000) Hz, number of $t_1$ increments = 256, acquisition time ($t_2$) = 256 ms, number of scans = 16. Data were zero-filled to 4 K (4 K) in $F_1$ ($F_2$) dimension, squared cosine window functions were applied in the $F_1$ and $F_2$ dimensions. Data were processed with the Felix97.0 software package (*36*).

iments due to its robust editing properties. However, since the chemical shift anisotropy of the $^{13}$C′ spin is quite large, the linewidth increases rapidly with magnetic field, resulting in a more insensitive experiment relative to the HN($\alpha/\beta$-NC′-*J*)-TROSY at the highest magnetic fields. In addition, since the chemical shift dispersion is usually smaller in the [$^{13}$C′, $^{1}$H] than in the [$^{15}$N, $^{1}$H] correlation spectrum, the H($\alpha/\beta$-NC′-*J*)CO experiment is not as suitable for large proteins as the HN($\alpha/\beta$-NC′-*J*) experiments.

In summary, in this paper we illustrate that filters selective to carbonyl carbon spin-states can be applied for the measurement of $^{1}J_{NC'}$ and $^{2}J_{HNC'}$ couplings from an [$^{15}$N, $^{1}$H] correlation spectrum processed to yield two simplified subspectra, each with no more cross peaks than a conventional decoupled [$^{15}$N, $^{1}$H]-HSQC spectrum. The HN($\alpha/\beta$-NC′-*J*) experiment implemented with the generalized TROSY scheme provides improved sensitivity and resolution at high magnetic fields. Alternatively, at intermediate field strengths, the spin-state-selective two-dimensional [$^{13}$C′, $^{1}$H] correlation spectrum is an

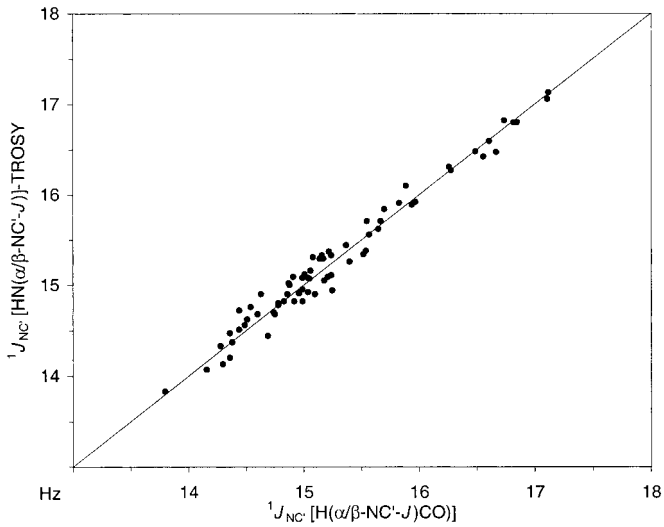


**FIG. 7.** Correlation plot of $^{1}J_{NC'}$ coupling constants measured with H($\alpha/\beta$-NC′-*J*)CO vs HN($\alpha/\beta$-NC′-*J*)-TROSY experiments for 69 residues in ubiquitin at 600 MHz, 25°C. The pairwise root-mean-squared deviation is 0.13 Hz.

attractive alternative to the HN($\alpha/\beta$-NC′-$J$) experiment. Generally, spin-state-selective spectral editing in two dimensions is most advantageous for larger proteins to provide orientational information with good resolution and sensitivity. These methods are also applicable to perdeuterated proteins.

## ACKNOWLEDGMENTS

This work was supported by the Academy of Finland.

## REFERENCES


1. C. Griesinger, O. W. Sørensen, and R. R. Ernst, *J. Am. Chem. Soc.* **107,** 6394 (1985).
2. C. Griesinger, O. W. Sørensen, and R. R. Ernst, *J. Chem. Phys.* **85,** 6837 (1986).
3. G. T. Montelione and G. Wagner, *J. Am. Chem. Soc.* **111,** 5474 (1989).
4. R. Weisemann, H. Rüterjans, H. Schwalbe, J. Schleucher, W. Bermel, and C. Griesinger, *J. Biomol. NMR* **4,** 231 (1994).
5. A. C. Wang and A. Bax, *J. Am. Chem. Soc.* **118,** 2483 (1996).
6. G. W. Vuister and A. Bax, *J. Am. Chem. Soc.* **115,** 7772 (1993).
7. H. Kuboniwa, S. Grzesiek, F. Delaglio, and A. Bax, *J. Biomol. NMR* **4,** 871 (1994).
8. A. Bax, D. Max, and D. Zax, *J. Am. Chem. Soc.* **114,** 6923 (1992).
9. J. R. Tolman and J. H. Prestegard, *J. Magn. Reson. B* **112,** 245 (1996).
10. R. Konrat, D. R. Muhandiram, N. A. Farrow, and L. E. Kay, *J. Biomol. NMR* **9,** 409 (1997).
11. G. Bodenhausen and D. J. Ruben, *Chem. Phys. Lett.* **69,** 185 (1980).
12. A. Bax, M. Ikura, L. E. Kay, D. A. Torchia, and R. Tschudin, *J. Magn. Reson.* **86,** 304 (1990).
13. F. Delaglio, D. A. Torchia, and A. Bax, *J. Biomol. NMR,* **1,** 439 (1991).
14. A. Meissner, J. Ø. Duus, and O. W. Sørensen, *J. Biomol. NMR* **10,** 89 (1997).
15. A. Meissner, J. Ø. Duus, and O. W. Sørensen, *J. Magn. Reson.* **128,** 92 (1997).
16. P. Andersson, K. Nordstrand, M. Sunnerhagen, E. Liepinsh, I. Turovskis, and G. Otting, *J. Biomol. NMR* **11,** 445 (1998).
17. P. Andersson, J. Weigelt, and G. Otting, *J. Biomol. NMR* **12,** 435 (1998).
18. K. Pervushin, R. Riek, G. Wider, and K. Wüthrich, *Proc. Natl. Acad. Sci. USA* **94,** 12366 (1997).
19. M. Salzmann, K. Pervushin, G. Wider, H. Senn, and K. Wüthrich, *Proc. Natl. Acad. Sci. USA* **95,** 13585 (1998).
20. P. Andersson, A. Annila, and G. Otting, *J. Magn. Reson.* **133,** 364 (1998).
21. M. Czisch and R. Boelens, *J. Magn. Reson.* **134,** 158-60 (1998).
22. A. Meissner, T. Schulte-Herbrüggen, J. Briand, and O. W. Sørensen, *Mol. Phys.* **95,** 1137 (1998).
23. M. Ottiger, F. Delaglio, and A. Bax, *J. Magn. Reson.* **131,** 373 (1998).
24. M. D. Sørensen, A. Meissner, and O. W. Sørensen, *J. Biomol. NMR* **10,** 181 (1997).
25. A. Bax, XVIII International Conference on NMR in Biol. Syst., Aug. 23–28, 1998, Hachioji, Tokyo.
26. O. W. Sørensen, G. W. Eich, M. H. Levitt, G. Bodenhausen, and R. R. Ernst, *Prog. NMR Spectrosc.* **16,** 163 (1983).
27. L. E. Kay, M. Ikura, R. Tschudin, and A. Bax, *J. Magn. Reson.* **89,** 496 (1990).
28. M. Goldman, *J. Magn. Reson.* **60,** 437 (1984).
29. M. D. Sørensen, A. Meissner, and O. W. Sørensen, *J. Magn. Reson.* **137,** 237 (1999).
30. A. Meissner, T. Schulte-Herbrüggen, and O. W. Sørensen, *J. Am. Chem. Soc.* **120,** 7989 (1998).
31. M. Piotto, V. Saudek, and V. Sklenar, *J. Biomol. NMR* **2,** 661 (1992).
32. M. McCoy and L. Mueller, *J. Am. Chem. Soc.* **114,** 2108 (1992).
33. A. J. Shaka, J. Keeler, T. Frenkiel, and R. Freeman, *J. Magn. Reson.* **52,** 335 (1983).
34. D. Marion, M. Ikura, R. Tschudin, and A. Bax, *J. Magn. Reson.* **85,** 393 (1989).
35. E. Kupce and R. Freeman, *J. Magn. Reson. A* **105,** 234 (1993).
36. FELIX 97.0, Biosym/MSI, San Diego, 1997.